LIDAR Validation Using GIS: A Case Study Comparison between Two LIDAR Collection Methods

Tim L. Webster
Department of Earth Sciences, Dalhousie University
and Applied Geomatics Research Group, Centre Of Geographic Sciences, Nova Scotia Community College
50 Elliot Road, RR#1
Lawrencetown, NS, Canada, B0S 1M0
E-mail: timothy.webster@nscc.ca

Abstract

In the summer of 2000, the Annapolis Valley of Nova Scotia, Canada was selected for a high-resolution elevation survey utilizing LIDAR (Light Detection And Ranging). Two different LIDAR systems were used to acquire data for the area. The vertical accuracy specification for the survey called for heights to be within an average of 15 cm of measured GPS heights and 95% of the data to be within 30 cm. Prior to the application of these data to geoscientific problems, extensive validation procedures were employed. High precision GPS and traditional surveys were conducted to collect height validation checkpoints. Two validation methods were developed in a GIS environment that involved comparing the checkpoints to the original LIDAR points and to an interpolated "bald earth" DEM. A systematic height error between flight lines for one of the LIDAR methods was detected that related to the calibration procedures used in the survey. This study highlights the differences between laser systems, calibration and deployment methodologies and emphasizes the necessity for independent validation data.

Introduction

LIDAR (Light Detection and Ranging) has been used for engineering, flood risk mapping (Webster *et al*. 2004) and it's utility has been demonstrated in forestry (Maclean & Krabill 1986), and glacier mass balance investigations (Krabill *et al*. 1995, 2000; Abdalati & Krabill 1999). A general overview of airborne laser scanning technology and principles is provided by Flood and Gutelius (1997) and Wehr and Lohr (1999). Applications to coastal process studies in the USA have been reported by Sallenger *et al*. (1999), Krabill *et al*. (1999), Brock *et al*. (2002), and Stockdon *et al*. (2002), among others. Preliminary trials in Atlantic Canada were reported by O'Reilly (2000) and subsequent studies were described by Webster *et al*. (2002, 2004 a). Various studies have been reported on the calibration and systematic errors of LIDAR systems (Kilian *et al*. 1996; Filin 2003) and the accuracy of laser altimetry data (Huising & Gomes Pereira 1998; Crombaghs *et al*. 2000; Maas 2000, 2002,). Although LIDAR technology has steadily improved since the mid-1990s, these studies highlight the requirement for height validation.

This paper describes a recent study where two data acquisition companies operating two different LIDAR sensors were contracted to acquire data for a large region of variable relief and land cover (Fig. 1). This provided an opportunity to compare two different acquisition methods using two different LIDAR systems. The vertical accuracy specification for the LIDAR surveys called for heights to be within an average of 15 cm of measured GPS heights and 95% of the data to be within 30 cm. The LIDAR data from the two methods and validation data were integrated into a GIS where two validation techniques were used for the analysis. The validation approaches for both LIDAR methods consisted of comparing checkpoints to both the original LIDAR points proximal to the checkpoints and to the derived "bald earth" DEM. The program code and details of the validation technique that compares the checkpoints to the proximal LIDAR points are described in detail elsewhere (see Webster and Dias submitted) and are summarized here. The focus of this paper will be on the LIDAR acquisition, GIS processing, and validation methods and results of LIDAR data acquired from the two different methods. The results indicate that one LIDAR method did not meet the specifications and had height discrepancies between flight lines as a result of a range bias that was related to the calibration procedures used. Although the other method met the specifications, LIDAR classification errors were identified that affected the validation results and the final DEM representation. This study demonstrates that differences in LIDAR systems and deployment methods yield different results, and implies that for any study, familiarity with the terrain, land cover, and climate is required in order to match the right LIDAR system to the right ground conditions. The requirement for

independent validation data and the development of validation techniques in the GIS environment proved to be critical in determining the accuracy of the different systems and the occurrence of a systematic range bias for one of the LIDAR methods.

LIDAR Acquisition Methods A and B

The study area is located on the southeast shore of the Bay of Fundy of Maritime Canada and includes the North Mountain and the South Mountain that bound the Annapolis Valley (Fig. 1). In addition to the acquisition of LIDAR, a variety of other remotely sensed data have been acquired and analyzed for this study area and are reported in Webster *et al*. (2004 b). The land use of the valley floor consists of agriculture and urban, while the North and South Mountains are mainly covered with dense mixed coniferous and deciduous forest.

Method A Survey

For LIDAR method A, the study area consisted of 350 km2 (Fig. 1). An Optech ALTM1020 sensor mounted in a Navajo P31 twin-engine fixed-wing aircraft was used in the survey. The LIDAR operated at a 5000 Hz laser repetition rate along with the scanning mirror operating at 15 Hz to direct the laser pulses across the swath. The system used a near-infrared laser operating at 1047 nm and has a beam divergence of 0.25 mrad (Fig. 2, A). The survey was conducted between July 6 and July 13, 2000 and consisted of 64 flight lines orientated parallel to the coast with two check lines running transverse to the coast. Since a "bald earth" DEM was one of the desired outcomes of the survey, the LIDAR unit was set to record the last return pulse. This increased the probability of getting a return from the ground or close to it in forested areas. The latest LIDAR sensors are capable of recording multiple returns, typically at least the first and last pulse with some sensors recording up to 4 intermediate returns, and in most cases the intensity of the reflected pulses (Toth 2004).

Method B Survey

For LIDAR method B, the study area consisted of 2,217 km^2 (Fig. 1). Unlike the Optech LIDAR system that combines the laser, GPS and IMU components into one package, this LIDAR system was originally designed for corridor data collection on a helicopter and was built from the individual components. The sensor was mounted on a pod that hung from a Bell Ranger 206 helicopter. The LIDAR operated at a 10,000 Hz laser repetition rate along with the scanning mirror operating at 15 Hz to direct the laser pulses across the swath. The mission was to be flown at an altitude of 900 m Above Ground Level (AGL), but due to an unforeseen reduction in laser power it was flown at 600 m AGL (Fig. 2, B). The survey was conducted between July 11 and August 31, 2000. This LIDAR system was only capable of recording the first return pulse.

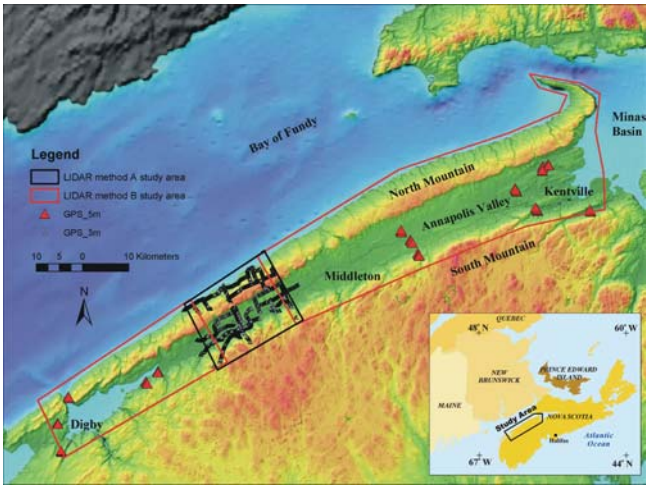

Figure 1 Colour shaded relief of 20 m DEM for the Annapolis Valley, Nova Scotia, highlighting the study areas of LIDAR methods A and B. Vehicle mounted real time kineamatic GPS measurements were used for study area A and static GPS measurements were used for study area B validation. The original 20 m DEM was produced by the Nova Scotia Geomatics Center, Service Nova Scotia & Municipal Relations. Location map inset in lower right shows the study area location in Maritime Canada.

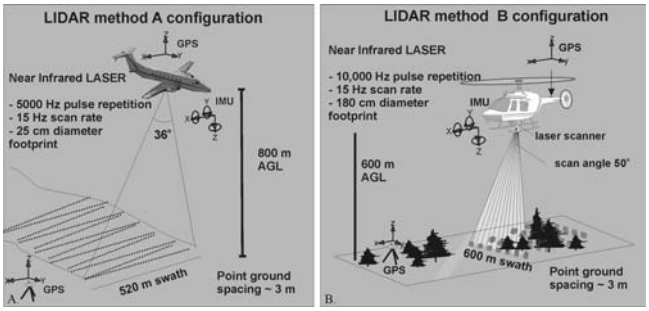

Figure 2 A LIDAR configuration for acquisition method A. B. LIDAR configuration for LIDAR acquisition method B.

GIS Processing and LIDAR Validation Methods

LIDAR data are typically delivered in ASCII files consisting of X,Y,Z data. The elevations were converted from ellipsoidal to orthometric heights above the geoid. In this case the HT_101 model supplied by the Canadian Geodetic Survey of Natural Resources Canada was used to relate WGS84 ellipsoidal heights to Canadian Geodetic Vertical Datum of 1928 (CGVD28). In addition to these fields we also acquired the GPS time stamp for every LIDAR return. This gives the ability to examine the LIDAR data by GPS time or flight line. Each survey method involved classifying the LIDAR point cloud into ground and non-ground points. Currently there is no standard format for LIDAR data, however the American Society of Photogrammertic Engineering and Remote Sensing (ASPRS)

recently published a proposed binary format that had several additional parameters such as scan angle for each LIDAR point (Schuckman, 2003).

The LIDAR points and ground validation points were imported into an Arc/Info GIS workstation running on a Unix platform. For LIDAR method A, each tile typically had in excess of 3 million points, of which over 1 million would typically be ground points. A "bald earth" DEM was constructed from the ground points of method A and used in part of the validation process. The 2 m resolution DEM was constructed by using a quintic (5^{th} order polynomial) interpolation method from the triangular irregular network (TIN) of the ground points. Several other interpolation methods were investigated such as spline techniques, inverse distance weighting, and kriging, in addition to the TIN method. Because of the relative uniform density of the ground points, although much higher in open areas than in the forest, the TIN and quintic interpolation method was selected because it best represented the ground surface with the fewest artifacts.

For method B however, there was a distinct lack of LIDAR points over low to moderate reflective near-infrared targets such as asphalt and coniferous forest as a result of the power reduction, although LIDAR returns with a ground spacing of 3 m were available for cleared grass covered areas. As a result of this, GPS collection concentrated on areas of grass fields where a dense coverage of LIDAR returns were guaranteed. The DEM constructed from the ground points from method B was not used in the validation because of the unreliability of the surface as a result of the sparse data points in many areas.

The absolute accuracy of LIDAR data depends on the removal of the systemic errors associated with the system. Filin (2003) provides an overview of the types and treatment for these sources of error in LIDAR systems. Kilian *et al*. (1996) described the methods of determining the local coordinates of LIDAR points by combining GPS, Inertial Measurement Unit (IMU), and the laser ranges, and measuring differences between strips. Maas (2000, 2002) improved this technique by implementing a method based on a Triangular Irregular Network (TIN) constructed from the LIDAR points for overlapping strips. Huising and Gomes Pereira (1998) reported on errors and accuracy of LIDAR data of the Netherlands collected by a variety of vendors using different systems. They observed height errors between strips that they attributed to GPS errors. Crombaghs *et al*. (2000) also observed errors near strip boundaries. Latypov and Zosse (2002) used overlapping strips to calibrate the parameters of the aircraft motion between strips, however ground control is required in order to perform a range calibration. These previous studies have dealt with relatively small study areas, compared to this study, and have been concerned with developing methods to resolve the relative differences between strips. As a result of that research, the issue of strip adjustment in LIDAR data has been highlighted as a potential source of error. In order to evaluate the possible error sources between strips, the GPS time tag for each LIDAR shot was used in the validation procedure as will be discussed in the next section.

The validation of the LIDAR was carried out in the GIS environment using two methods:

1. Ground validation points were compared to proximal LIDAR points, and
2. Ground validation points were compared to the DEM derived from LIDAR ground points.

For all validation datasets the orthometric heights have been computed using the HT1_01 model to allow direct comparison with the LIDAR orthometric heights. For validation method 1, an automated procedure was coded in the Arc Macro Language (AML) that involved a user specified horizontal search radius, typically less than 5 m, around the validation point and all LIDAR ground points within that area were selected and orthometric heights were compared to that of the validation point. The details of the program are described elsewhere and the AML code is available for download (see Webster and Dias submitted). For LIDAR method A, Real Time Kinematic (RTK) GPS validation points were collected from a moving vehicle on the road and the search radius was restricted to 3 m (Fig. 1). A Leica system 530 was used to collect the RTK GPS data with points collected within a maximum of 12 km from base stations to minimize errors. In general the carrier phase differential GPS real time data had a height precision smaller than 5 cm. For LIDAR method B, static carrier phase differential GPS validation points were collected in flat grass fields and a search radius of 5 m was used to ensure a sufficient sample of LIDAR points (Fig. 1). Trimble single frequency (4600) and dual frequency (4000) GPS receivers were used in this survey and baselines were kept below 10 km with observation times greater than 1 hour. The reported vertical error (one standard deviation) of these GPS data was smaller than 3 cm. With the validation method that compares proximal LIDAR points to GPS points, two types of tables are produced within the GIS. One table summarized the statistics of the LIDAR points for each GPS validation point and the second table contains information for each LIDAR point that occurs within the specified radius of the validation point and includes the difference in height and horizontal distance between the points.

For validation method 2, the validation points are overlain on the gridded DEM surface and the cell value of the DEM is compared to the validation point's orthometric height. This method rapidly gives an assessment of the accuracy of the DEM product that was derived from the LIDAR ground points.

The combination of using both validation methods to determine possible LIDAR ground point classification errors is described in the results section.

Results

LIDAR Method A

For LIDAR method A, both validation techniques were used: analysis of the LIDAR ground points and of the

interpolated DEM. Only RTK GPS points with reported height precision less than 5 cm were used based on one standard deviation. A total of 12,675 GPS RTK points were collected on the road and used with a 3 m search radius to extract LIDAR ground points. The summary statistics for the LIDAR ground points within 3 m of the GPS points is presented in figure 3, A. From the summary statistics these data have met the vertical specification, with a mean (ΔZ = GPS - LIDAR heights) less than 15 cm, however only 93.5 % of the LIDAR data are within 30 cm of GPS points. Of the original 12,675 GPS points, only 11,853 points had LIDAR ground points within 3 m. Averaging the ΔZ values of proximal LIDAR points for each of the GPS points results in 98.9% of the GPS data being within 30 cm (Fig. 3, B).

Derivative products from the LIDAR points, such as DEMs, are commonly used for subsequent analysis and deriving information about geologic and geomorphic features. Therefore an analysis of the LIDAR-derived DEM is useful and ensures every GPS point is used in the comparison because a continuous surface is constructed from the LIDAR ground points. The 12,675 GPS points were overlain on the DEM and the corresponding cell values extracted and compared. The summary statistics for this analysis is presented in figure 3 (C). Many of the GPS locations that have a ΔZ > 30 cm, which are indicated in figure 3 (C), were not included in the previous analysis because no LIDAR ground points were within 3 m of the GPS points. This situation commonly occurs at small bridges and other steep rises of the roadbed where the LIDAR points have been misclassified as non-ground (Fig. 4). As a result, the DEM is too low for these areas and the roadbed is not properly represented because LIDAR points either side of the road have been classified as ground and used to construct the DEM (Fig. 4). The top map in figure 4 shows the GPS points colour-coded by ΔZ (GPS-LIDAR DEM), and the lower map shows the GPS points colour-coded by the mean ΔZ (GPS-LIDAR points within 3 m of GPS points). The red points in the top map (Fig. 4, A) are absent from the bottom map because no LIDAR ground points were within 3 m of those GPS points (Fig. 4, B). This means that the ΔZ statistics generated from the first validation method did not include these errors (Fig. 3, A). Thus, the combination of both validation methods (GPS compared to LIDAR points within a radius and GPS compared to the DEM surface) also highlight where the LIDAR classification algorithm may have misclassified LIDAR points as non-ground when they truly represented ground features such as the elevated roadbed. By comparing all the GPS points to the DEM cell values (Fig. 5), 95% of the GPS points have a ΔZ less than 30 cm. In figure 5 the red GPS points highlight possible LIDAR point classification errors and correspond to the large positive values in ΔZ in figure 3 (C), where the DEM surface is too low. The

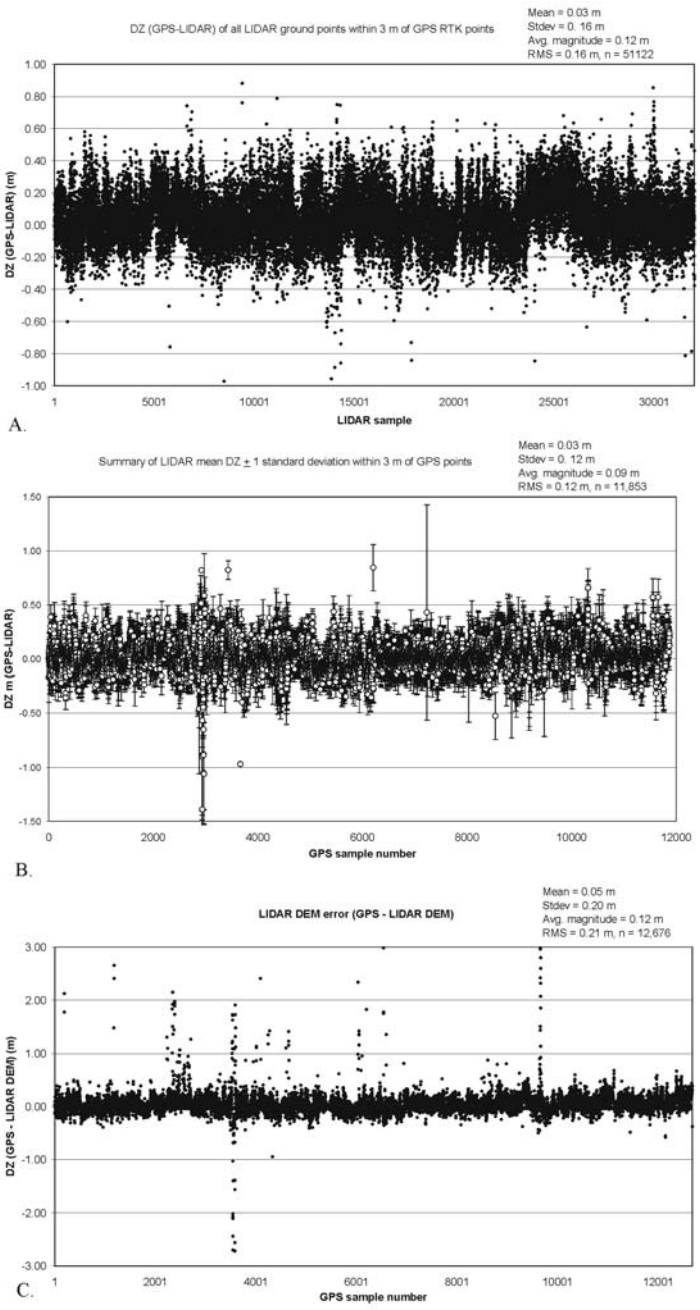

Figure 3 A. Graph of ΔZ for all the LIDAR ground points within 3 m of GPS RTK points for LIDAR method A. The mean difference in ΔZ is 0.03 m, with a mean magnitude of 0.12 m, a standard deviation of 0.16 m, and a RMS error of 0.16 m, n = 51,122; 93.5% of the LIDAR points are within 30 cm of the GPS points. Note ΔZ is denoted DZ on the graph.

B. Graph of the mean value of ΔZ + one É„Énerror bars for each GPS validation point for LIDAR method A. The mean difference in ΔZ is 0.03 m, with a mean magnitude of 0.09 m, a standard deviation of 0.12 m, and a RMS error of 0.12 m, n = 11,853; 98. 9% of the GPS points are within 30 cm of the mean of the LIDAR points. Note ΔZ is denoted DZ on the graph. C. Graph of ΔZ (GPS-LIDAR DEM) for the GPS validation points compared to the LIDAR DEM surface for LIDAR method A. The mean difference in ΔZ is 0.05 m, with a mean magnitude of 0.12 m, a standard deviation of 0.2 m, and a RMS error of 0.21 m, n = 12, 676; 95% of the GPS points are within 30 cm of the LIDAR DEM surface. Note ΔZ is denoted DZ on the graph.

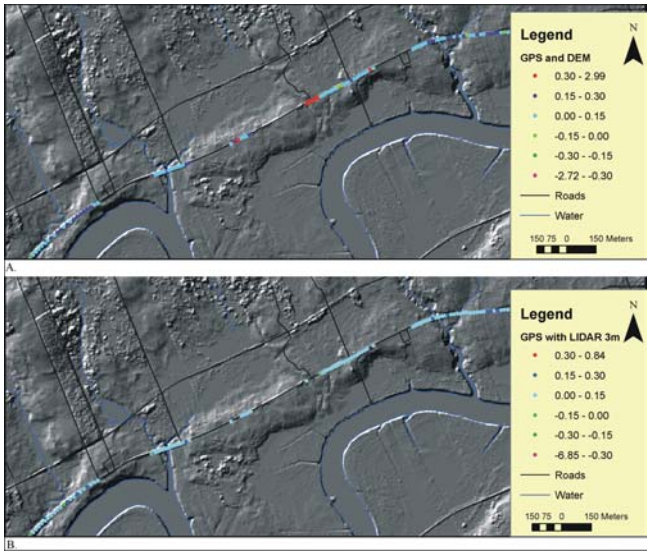

Figure 4 A. The GPS points colour-coded based on ΔZ (GPS-LIDAR DEM) overlaid on the shaded relief LIDAR DEM.
B. The GPS points that have LIDAR ground points within 3 m and are colour-coded based on the mean ΔZ (GPS-LIDAR) overlaid on the shaded relief LIDAR DEM.
Note the points that exceed 30 cm in the top map (A) are absent in the lower map (B) as a result of the LIDAR points in these areas being classified as non-ground. Note ΔZ is denoted DZ on the graph.

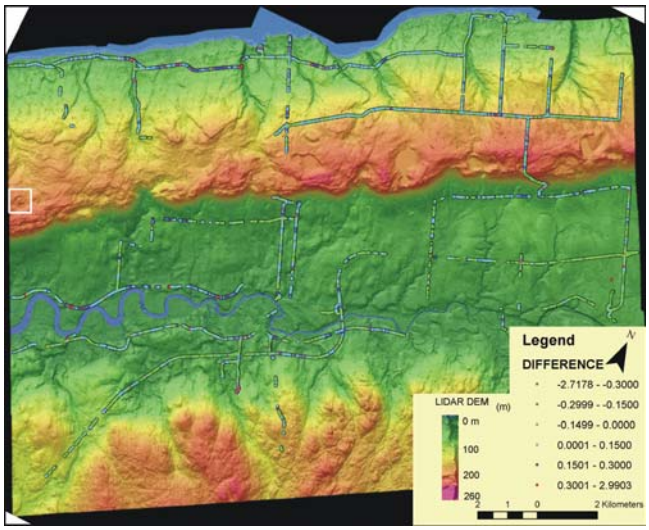

Figure 5 GPS points colour-coded by ΔZ (GPS-LIDAR DEM) overlaid on the colour shaded relief DEM derived from the ground LIDAR points. The white square inset in the upper left section of the image indicates the location of the transects under the forest canopy (Fig. 6). The graph of ΔZ and associated statistics of these GPS points is presented on figure 3, C. Most of the GPS points indicating error in the LIDAR DEM occur in valleys or depressions where the road surface is too low in the DEM as a result of LIDAR points along the road being classified as non-ground.

graph of ΔZ for all LIDAR ground points within 3 m of GPS points (Fig. 3, A) is symmetric about zero, with no significant large ΔZ values, because no LIDAR points classified as ground occur around those GPS points.

The issue of ground points being classified as non-ground occurs in other cases that are important from a geologic and geomorphic interpretation of the LIDAR-derived DEMs. Two cases encountered with this dataset included the roofs of large buildings being classified as ground and the tops of cliffs both along the coast and the cuesta of the North Mountain being classified as non-ground. Both situations can result in a DEM that does not accurately represent the landscape and can lead to possible erroneous interpretations. These types of misclassification errors for structures with steep slopes must be found and properly classified prior to building the DEM.

High precision GPS cannot produce accurate results under the forest canopy and validation of the LIDAR-derived DEM in this environment is more difficult. A topographic survey consisting of two transects utilizing a Leica total station was conducted under the canopy. The site for the survey was selected in order to investigate a geomorphic ring structure that is visible on the "bald earth" DEM (Fig. 5, 6). The structure is completely covered by forest with the exception of a small wetland on the eastern edge and a forest clear-cut to the west (Fig. 6, A). From these open areas GPS control was established for the transects. The southwest-northeast trending transect consisted of 146 points with a mean ΔZ between the survey heights and the interpolated DEM heights of -0.1 m, a mean magnitude of error of 0.24 m, a standard deviation of 0.3 m, and a RMS error of 0.32 m (Fig. 7, A). The southeast-northwest trending transect consisted of 102 points and had a mean ΔZ of -0.13 m, a standard deviation of 0.37 m, and a RMS error of 0.39 m (Fig. 7, B). In general, both transects had LIDAR-derived DEM values slightly higher than the survey heights. These differences are interpreted to be a result of LIDAR returns off of shrubs being classified as ground, thus causing the DEM surface to be a few decimeters higher in places than the actual ground (see Webster and Dias submitted for details of LIDAR point analysis).

LIDAR Method B

The reduced laser power during this survey resulted in LIDAR returns only from highly reflective targets such as deciduous trees and grass. As a result, most roads, buildings, and coniferous forest stands were absent from the dataset. To ensure a large sample of LIDAR ground returns for the validation analysis, GPS data were acquired in a systematic pattern across the LIDAR swaths in open flat grass covered fields (Fig. 1). As a result of the missing ground points over dark targets the resultant DEM was of limited use, therefore only validation method 1 was used with these data. A total of 51 post processed phase differential static GPS points were used and a 5 m horizontal search radius was specified around these points, resulting in 970 ground LIDAR points for comparison (Fig. 1, 8).

The mean difference in orthometric heights between the LIDAR and validation points was 1.18 m with a standard deviation of 0.64 m and a RMS error of 1.34 m (Fig. 8). As can be seen in figure 8, there is a large spread in ΔZ and the

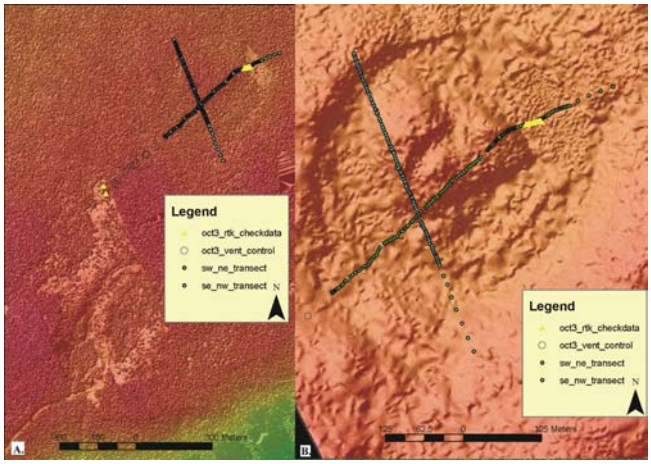

Figure 6 Location of the ring structure and transects.
A. This map represents a Digital Surface Model (DSM) derived from all the LIDAR points (ground and non-ground). A road leading to a forest clear-cut is present near the center of the map. This clear cut allowed for GPS data to be collected and used as control for the two forested transects utilizing a total station survey.
B. The map on the right is at a larger scale and represents the "bald-earth' DEM of the ring structure and associated transect locations.
Notice how the structure is not visible in the DSM (A) and is apparent in the DEM (B). The yellow triangles represent the GPS control (west in the clear cut) and check data (east in the wetland) and the other points represent the total station survey data.

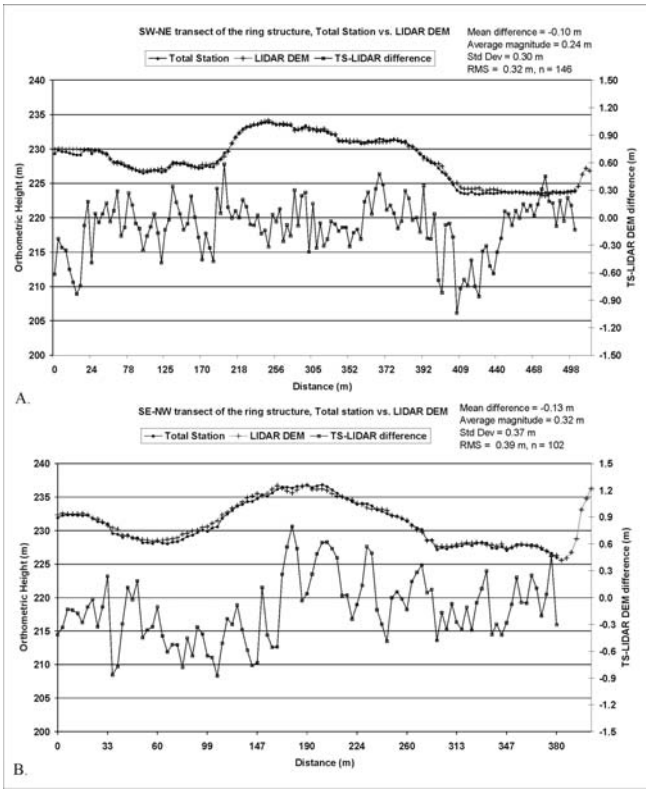

Figure 7 A. Plot of the southwest-northeast trending transect across the ring structure. Total station survey points are denoted by black dots and black crosses denote the LIDAR DEM points. The height difference between the total station survey and LIDAR DEM is plotted as open squares and corresponds to the scale on the right y-axis of the graph. The mean ΔZ is -0.1 m, with an average magnitude of 0.24 m, a standard deviation of 0.30 m and a RMS error of 0.24 m. Note ΔZ is denoted DZ on the graph. B. Plot of the southeast-northwest trending transect across the ring structure. The mean ΔZ is -0.13 m, with an average magnitude of 0.32 m, a standard deviation of 0.37 m and a RMS error of 0.39 m. Note ΔZ is denoted DZ on the graph.

values appear clustered for different elevations with variable ranges but no systematic pattern. The summary statistics indicate these LIDAR data do not meet the vertical specifications. The GPS ΔZ (GPS-LIDAR) standard deviation focuses attention on where the LIDAR data shows the most differences with the validation data and can be further examined (Fig. 9). For example, GPS sample number 19 has a ΔZ standard deviation of 1.35 m. The relationship between the height differences (ΔZ) of GPS point 19 and the 38 surrounding LIDAR points within 5 m appears random (Fig. 10, A). However, if ΔZ is plotted against GPS time, the time the LIDAR was collected, there are two distinct populations of ΔZ, from -1.47 to 1.20 m and from 1.44 m to 3.4 m (Fig. 10, B). Each distinct range of ΔZ is associated with a different LIDAR GPS collection time that is in turn related to different flight lines. The time between LIDAR point acquisitions for this case is on the order of 1903 seconds or 30 minutes indicating the LIDAR points were collected in two different flight lines. When the LIDAR points are colour-coded by the GPS time tag the two flight lines are evident, and when the LIDAR points are colour-coded by ΔZ, the spatial relationship between ΔZ and each flight line becomes apparent. This systematic height bias between flight lines was evident in all of the GPS checkpoints that were collected. It was determined that the source of the vertical error was related to a range bias. This range bias was not correctly compensated for in the calibration procedures used during the survey. The LIDAR

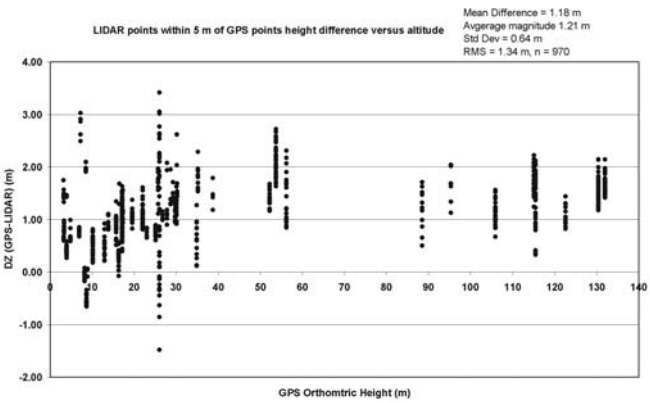

Figure 8 Graph of ΔZ (GPS-LIDAR) of all LIDAR ground points for method B within 5 m of GPS points versus the orthometric height. The mean ΔZ is 1.18 m, with an average magnitude of 1.21 m, a standard deviation of 0.64 m and a RMS error of 1. 34 m. Note ΔZ is denoted DZ on the graph.

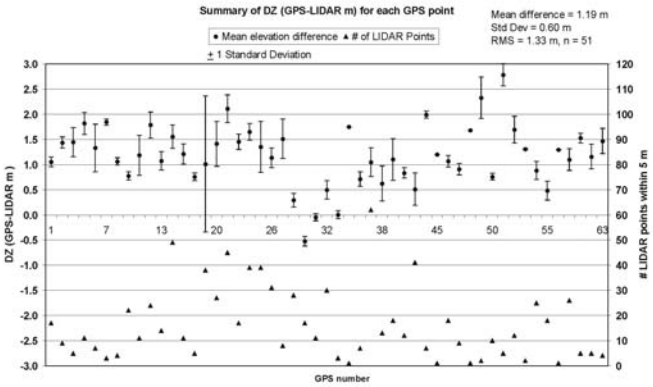

Figure 9 Graph of GPS points summary statistics of elevation differences with the surrounding LIDAR ground points for LIDAR method B. The mean ΔZ for each GPS point is denoted by black dots + one É„Énerror bars, and the number of LIDAR points within 5 m of each GPS point is denoted by the black triangles. The number of LIDAR points associated with each GPS point is defined by the right y-axis. The mean ΔZ is 1.19 m, a standard deviation of 0.60 m and a RMS error of 1.33 m. Notice GPS point 19 (Digby area) has a large standard deviation of 1.35 m and 38 associated LIDAR points. Note £GZ is denoted DZ on the graph.

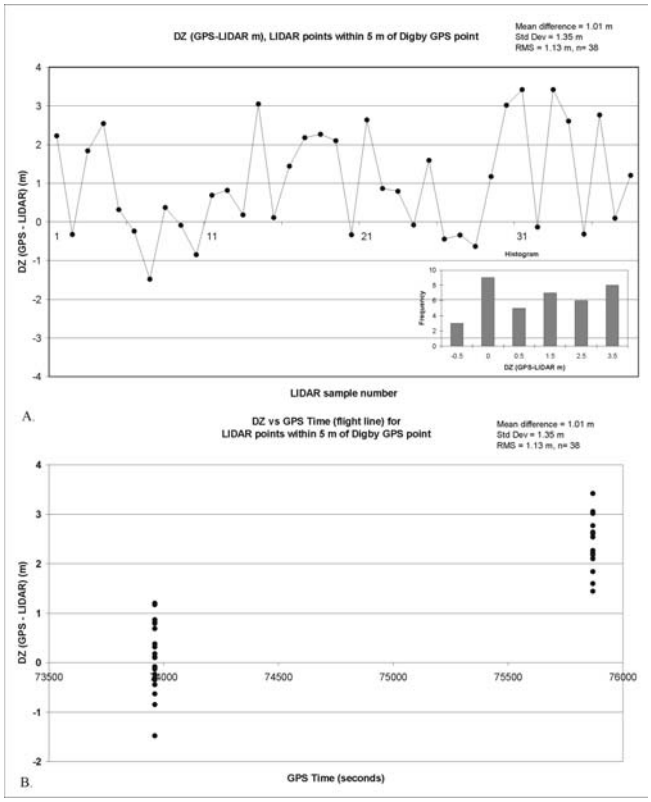

Figure 10 A. Graph of the 38 LIDAR points ΔZ associated with GPS sample point number 19 for the Digby area. There is no apparent systematic pattern to ΔZ. The lower right inset histogram shows a near equal distribution of ΔZ from -0.5 to 3.5 m. Note ΔZ is denoted DZ on the graph. B. Graph of the LIDAR points ΔZ versus GPS acquisition time associated with GPS validation point number 19. The ΔZ values appear to be related to the GPS time, each flight line has a different ΔZ range associated with it. Note ΔZ is denoted DZ on the graph.

calibration procedure employed at that time involved flying at the planned survey height of 900 m and acquiring LIDAR points over the GPS base station located at the airport. From this procedure the raw laser ranges of the unit were calibrated. However, as a result of the power reduction of the laser, the actual flying height was reduced to approximately 600 m altitude during the actual survey, introducing a range bias that was not compensated for. To verify this, several lines of LIDAR data were reprocessed with the appropriate scale factor and offset for the lower altitudes and matched the validation data more closely. Since the dataset was of limited value because of the sparse distribution of the points over dark targets as a result of the power reduction, the remainder of the data was not reprocessed; rather the study area was resurveyed in 2003-2004 with leaf-off conditions using a LIDAR with several improvements. A collimator was attached to the head of the laser having the effect of narrowing the beam divergence to smaller than 0.3 mrad. This resulted in the laser footprint being reduced from 180 cm to 18 cm. Although not tested directly, the smaller ground footprint of the laser beam should improve the horizontal accuracy of the system as well. Preliminary analysis indicates these data meet the vertical specifications.

Summary and Conclusions

This study demonstrates the importance of independent detailed validation data in order to ensure the LIDAR data meet the high accuracy specifications. With LIDAR vertical specification requirements of 15 cm on average and 95% of the data to be within 30 cm of measured GPS points requires validation data that exceeds this accuracy. The data from both LIDAR methods had extra data fields consisting of the GPS time tag for each LIDAR shot. This proved to be a very valuable attribute to enable the LIDAR points to be separated based on time and flight line, thereby facilitating comparisons with the vertical characteristics of the data between flight lines. In the case of method A, the vertical accuracy specifications were met, although misclassification errors were observed. In the case of method B, problems were encountered during the survey that resulted in a power reduction of the laser system and LIDAR ground points were absent for many dark targets. Method B did not meet the vertical accuracy specifications and the source of the vertical error related to a range bias that was not compensated for in the calibration procedures. The original survey was planned at an altitude of 900 m, however as a result of the power loss, the actual survey was flown at altitudes closer to 600 m. The change in flying height introduced range errors that were not accounted for. A range bias and scaling factor were computed and applied to some of the flight lines for confirmation.

A total station topographic survey was conducted in a mixed forest area where a ring structure with topographic relief on the order of about 10 m over a distance of 500 m was observed. Overall the RMS error under the canopy was about 10 cm larger than the validation results on the roadbed and was attributed to ground vegetation returns. However, the

details of the profile generated from the DEM match that of the survey data sufficiently to consider the information from the DEM reliable for use in geological mapping and interpretation.

Specific conclusions that can be drawn from this study include:

1. When planning a LIDAR survey, familiarity with the terrain and landcover characteristics of the study area is necessary in order to select the most appropriate LIDAR system. This study shows that not all LIDAR systems are suited for all terrain conditions. For example, in the case of single return systems, a first return only system is suitable for areas of sparse vegetation, while a last return system is more appropriate for densely vegetated areas. The beam divergence and pulse repetition rate must also be considered in this context. For a first return system to measure the ground in vegetated terrain, a very narrow ground laser footprint is desired. The beam divergence will also influence the strength of the returning signal. This was evident during the repeat survey of method B when the beam divergence was reduced from a ground footprint of 180 cm to 18 cm diameter. However, if a last return system is used, a moderate beam footprint is desired so that some of the incident energy will make it past holes in the canopy and be reflected off the ground. In both cases the higher the laser pulse repetition rate the more total points there are, thus more points will make it to the ground, although this will increase the data volume.
2. Accurate classification of the LIDAR point cloud into ground and non-ground points is important for detailed geomorphic analysis. In this study the problem of misclassification was demonstrated with the raised roadbed. Current classification algorithms code points as being non-ground if they exceed a variance threshold for a neighborhood of points. Natural terrain breaks such as cliffs and nick points in stream profiles are subject to misclassification because of this. The data must be examined critically to check for such classification errors. The combination of the two validation methods facilitated the identification of these problems along the road. Improved point classification is an area of current research in the LIDAR community.
3. The selection of the season to conduct the survey is important for vegetated terrain and depends on the local climate. The detection of the ground in conditions of leaf-on and dense shrub and ground vegetation are problems for LIDAR systems. Leaf-off conditions are desired if a "bald-earth" DEM is the main purpose of a LIDAR survey. However, winter acquisitions present the problem of variable snow depths due to drifting. Thus the spring and fall time periods present the best alternatives. Of these periods, the spring has the added benefit of reduced shrub and under story vegetation height as a result of flattening by the winter snow pack. In this study the problem of shrub vegetation representing ground elevations was demonstrated in the validation work under the forest canopy for the ring structure.
4. Independent high precision validation data is required in order to check the vertical accuracy of the LIDAR data. Proper LIDAR sensor calibration procedures must be employed in order to remove systematic errors that are present in the data when it is collected. As demonstrated in this study, insufficient calibration procedures resulted in a range bias that manifested itself as height differences between flight lines.
5. The use of GIS for automated validation procedures. In this study a large area of LIDAR data was collected resulting in a voluminous amount of data to be processed. The ability to automate validation procedures that examine the check data against the original LIDAR points and the derived DEM facilitates the identification of errors. As demonstrated here, the two techniques compliment one another in identifying errors related to misclassification (e.g. roadbed surface classified as non-ground) and range bias.
6. The addition of the GPS time tag or a flight line identifier in the LIDAR data is extremely useful for validation purposed. Without such a field it would be very difficult to identify systematic errors between flight lines such as the range bias identified and described in this study.

Acknowledgements

This study benefited from the contribution of several people. I would like to thank the financial assistance of Brendan Murphy, St. FX University and the Nova Scotia Community College (NSCC) towards my PhD. I would like to thank the support of my thesis committee consistsing of Brendan Murphy, John Gosse, and Ian Spooner. I would also like to thank Dennis Kingston and the AGRG students involved in some of the validation data collection: Paul Fraser and Dan Deneau for the 2001 rapid static GPS survey, and Trevor Milne and the students from the AGRG class of 2003-2004 for the total station survey. Also, George Dias for writing the AML code for the first validation procedure and Lisa Markham and Dan Deneau for assisting in parts of the AML. Special thanks to Bob Maher and David Colville of the AGRG, and Don Forbes of the Geological Survey of Canada for their support and constructive comments during the project. The LIDAR data for this project was funded by an infrastructure grant to NSCC from the Canadian Foundation for Innovation, Industry Canada. I would like to thank an anonymous reviewer who's suggestions and comments have improved the manuscript.

References

Abdalati, W. and Krabill, W.B. 1999. *Calculation of ice velocities in the Jakobshavn Isbrae area using airborne laser altimetry*. Remote Sensing of the Environment 67: 194-204.

Brock, J.C., Wright, C.W., Sallenger, A.H., Krabill, W.B. and Swift, R.N. 2002. *Basis and methods of NASA airborne topographic mapper LIDAR surveys for coastal studies*. Journal of Coastal Research 18: 1-13.

Crombaghs, M., Bruelgelmann, R., and E.J. deMin. 2000. *On the adjustment of overlapping strips of laser altimeter height data*. International Archives of Photogrammetric Engineering and Remote Sensing 33 (B3/1): 230-237.

Filin, S. 2003. *Recovery of Systematic Biases in Laser Altimetry Data Using Natural Surfaces*. Photogrammetric Engineering & Remote Sensing 69, no. 11: 1235-1242.

Flood, M. and Gutelius, B. 1997. *Commercial implications of Topographic Terrain Mapping Using Scanning Airborne Laser Radar*. Photogrammetric Engineering and Remote Sensing 4: 327-366.

Huising, E.J. and Gomes Pereira, L.M. 1998. *Errors and accuracy estimates of laser data acquired by various laser scanning systems for topographic applications*. ISPRS Journal of Photogrammetric Engineering and Remote Sensing 53, no. 5: 245-261.

Kilian, J., Haala, N., and Englich, M. 1996. *Capture and evaluation of airborne laser scanner data*. International Archives of Photogrammetric Engineering and Remote Sensing 31 (B3): 383-388.

Krabill, W., Abdalati, W., Frederick, E., Manizade, S., Martin, C., Sonntag, J., Swift, R., Thomas, R., Wright, W. and Yungel, J. 2000. *Greenland Ice Sheet: high-elevation balance and peripheral thinning.* Science 289: 428-430.

Krabill, W.B., Thomas, R.H., Martin, C.F., Swift, R.N. and Frederick, E.B. 1995. *Accuracy of airborne laser altimetry over the Greenland ice sheet*. International Journal of Remote Sensing 16: 1211-1222.

Krabill, W.B., Wright, C., Swift, R., Frederick, E., Manizade, S., Yungel, J., Martin, C., Sonntag, J., Duffy, M. and Brock, J. 1999. *Airborne laser mapping of Assateague National Seashore Beach*. Photogrammetric Engineering & Remote Sensing 66: 65-71.

Latypov, D., and Zosse, E. 2002. *LIDAR data quality control and system calibration using overlapping flight lines in commercial environment*. Proceedings of the American Society of Photogrammetry and Remote Sensing Annual Conference, Washington, D.C., pp 13.

Maas, H.G. 2000. *Least-Squares Matching with Airborne Laserscanning Data in a TIN Structure*. International Archives of Photogrammetric Engineering and Remote Sensing 33 (B3/1): 548-555.

Maas, H.G. 2002. *Methods for Measuring Height and Planimetry Discrepancies in Airborne Laserscanner Data*. Photogrammetric Engineering & Remote Sensing, 68, no. 9: 933-940.

Maclean, G.A. and Krabill, W.B. 1986. *Gross-merchantable timber volume estimation using an airborne LIDAR system*. Canadian Journal of Remote Sensing 12: 7-18.

O'Reilly, C. 2000. *Defining the coastal zone from a hydrographic perspective*. Proceedings, Workshop on risk assessment and disaster mitigation: Enhanced use of risk management in integrated coastal management. International Ocean Institute, Bermuda. Backscatter, April 2000, pp. 20-24

Sallenger, A.B., Jr., Krabill, W., Brock, J., Swift, R., Jansen, M., Manizade, S., Richmond, B., Hampton, M. and Eslinger, D. 1999. *Airborne laser study quantifies El Nino- induced coastal change*. Eos, Transactions, American Geophysical Union, 80: 89, 92.

Schuckman, K. 2003. *Announcement of the Proposed ASPRS Binary Lidar Data File Format Standard*. Photogrammetric Engineering & Remote Sensing 69, no. 1:13-19.

Stockdon, H.F., Sallenger, A.H., List, J.H. and Holman, R.A. 2002. *Estimation of shoreline position and change using airborne topographic LIDAR data*. Journal of Coastal Research 18, no. 3: 502-513.

Toth, C.K. 2004. *Future Trends in LIDAR*. Proceedings of American Society of Photogrammetric Engineering and Remote Sensing Annual Conference, May 2004.

Webster, T.L., and Dias, G. submitted. *LIDAR validation using GIS: An automated procedure for comparing GPS and proximal LIDAR ground elevations*. Computers & Geosciences.

Webster, T.L., Forbes, D.L., Dickie, S., 2004. *Using topographic lidar to map flood risk from storm-surge events from Charlottetown, Prince Edward Island*. Canadian Journal of Remote Sensing 30, no. 1: 64-76.

Webster, T.L., Christian, M., Sangster, C. and Kingston, D. 2004. *High-Resolution Elevation and Image Data Within the Bay of Fundy Coastal Zone, Nova Scotia, Canada*. In GIS for Coastal Zone Management. Edited by Bartlett, D. and Smith, J., CRC Press.

Webster, T.L., Forbes, D.L., Dickie, S., Colville, R. and Parkes, G.S. 2002. *Airborne imaging, digital elevation models and flood maps*. In Coastal impacts of climate change and sea-level rise on Prince Edward Island. Edited by Forbes, D.L. and Shaw, R.W. Geological Survey of Canada Open File 4261, Supporting Document 8, 36 p. (on CD-ROM).

Wehr, A. and Lohr, U. 1999. *Airborne laser scanning - An introduction and overview*. Journal of Photogrammetry and Remote Sensing 54: 68-82.